Neutral Current Optimization Control for Smart Transformer-fed Distribution System under Unbalanced Loads

Junru Chen, *Membere, IEEE,* Rongwu Zhu, *Member, IEEE,* Ismail Ibrahim, *Student member IEEE,* Terence O'Donnell, *Member, IEEE,* Marco Liserre, *Fellow, IEEE* [1]

***Abstract*—In a 3-phase 4-wire LV distribution system, unbalanced loads lead to neutral current (NC) looping resulting in increase of power losses and variation of neutral potential. Compared to the conventional power transformer, Smart Transformer (ST) has strict current limitations to avoid overcurrent. However, its advantages on the downstream LV grid voltage regulation can provides the capability to regulate excessive NC. This paper proposes a closed-loop NC optimization control in order to, on the one hand, minimize the NC current in the normal operation satisfying the standard EN 50160 requirement, on the other hand, suppress the NC current in extreme cases to avoid the overcurrent damage of the ST. The proposed control strategies are validated by experimental tests via the hardware-in-the-loop setup and a case study based on a 350kVA, 10kV/400V, ST-fed distribution network under unbalanced loading profile according to the 3-phase 4-wire distribution grid in Manchester area. The results clearly prove the effectiveness and flexibility of the proposed NC optimization control strategies on the NC suppression and minimization.**

Keywords—Smart Transformer, Neutral Current Control, Unbalanced Load, Voltage Unbalance Degree Limitation

I INTRODUCTION

The increase in the application of the power electronics converters in the grid has the potential to make the grid more flexible and smarter. The power electronics based smart transformer (ST) [1] has been proposed as an alternative to the conventional distribution transformer in this smart grid. The ST, can have multiple DC and AC ports connecting to different subsystem [2], e.g. renewable generation [3], electrical storage [4,5], or electrical vehicle charging station [6], can provide an interface between transmission and distribution systems [1], and act as a hub to centrally regulate the power flow between these subsystems [7].

Based on its control possibilities, the ST can provide auxiliary services to the grid which might otherwise have to be provided from other sources and devices. For example, using the decoupled voltage and fast response features, the ST can provide accurate real-time measurement of the load state, such as load voltage sensitivity [8] and load frequency sensitivity [9]. This dynamic load identification can help the ST regulate the load dynamically in order to achieve, for example, demand minimization [10] and system frequency support [11]. In addition, the decoupled reactive power at the primary side can be used to support upstream system voltage through reactive power compensation [12].

However, compared with a conventional transformer, the ST has lower efficiency, up to 96.7% [13,14] and has strict current limitations to avoid overload damage [15]. Use of the ST therefore only becomes feasible if its control possibilities can reduce overall system losses and limit currents. In 3-phase 4-wire distribution networks, the connected loads are stochastically unbalanced. The resulting unbalanced load current flows in the neutral line causing a certain neutral current (NC). In some occasions, the NC can even exceed the phase current [16], potentially leading to overcurrent in the ST. In addition, the NC represents a power loss and causes voltage drop which impacts on the load voltage [17]. Therefore, a proper NC control approach would have a benefit for both the distribution system and the connected ST.

Conventionally, in order to suppress the excessive NC, extra power converters-based devices, such as the active power filter (APF) [18-20] and hybrid power conditioner (HPC) [21-23] have been adopted to coordinate with the conventional transformer and to reduce the NC by eliminating triple harmonics, at the point of connection of the nonlinear or unbalanced load. In contrast to those approaches, the work described in this paper assumes that an ST is feeding a network largely composed of single phase loads which are overall unbalanced and it proposes a control technique which can be integrated with the ST so as to reduce NC from the source side. The work in this paper directly addresses fundamental component NC, as opposed to that arising from triple harmonics which can also be eliminated in a converter-fed system, such as [24 – 26].

Some NC control approaches in fundamental frequency have been proposed for the ST-fed system. The basic idea is to purposely unbalance the load supply voltage phase and/or amplitude so as to cancel the current unbalance due to the unbalanced loads. The objective of the fundamental NC control

This work is funded by the Science Foundation Ireland (SFI) Strategic Partnership Programme Grant Number SFI/15/SPP/E3125, the SFI Grant Number SFI/16/IA/4496 and the European Research Council (ERC) under grant 616344 HEART

Junru Chen, Ismail Ibrahim and T. O'Donnell are with the Electrical Engineering Department, University College Dublin, Dublin 4, Ireland (e-mail: junru.chen.1@ucdconnect.ie; ismail.ibrahim@ucdconnect.ie; tenrence.odonnell@ucd.ie).

R. Zhu and M. Liserre are with Kiel University, Kiel, Germany (e-mail: rzh@tf.uni-kiel; ml@tf.uni-kiel.de).

is the reference voltage but not the modification on the voltage or current control loop, so that it does not conflict with and can coordinate with those harmonic elimination methods. Reference [27,28] proposed a method for application in data centres to fully eliminate the NC. However, the voltage unbalance required is significant so that it cannot be applied in the distribution system. The public distribution grid standard EN50160 [29] specifies that the voltage unbalance degree should be less than 2% over 95% of the time. Considering these voltage operation limits, reference [30] proposes a NC minimization approach, which although it cannot eliminate the NC it can still achieve approximately 10% NC reduction. Since the relationship amongst the voltage unbalance, load unbalance and NC is nonlinear, the realization of this method is based on linearization of this relationship by introducing a constant parameter in the control scheme corresponding to the 2% voltage unbalance limit. The introduced parameter sets a narrow bound to the movement of the control and thus degrades the robustness of the control. The most drawback of these previous methods is that it did not provide closed loop control on the NC limitation. Reference [31] firstly uses the feedback NC to reduce the NC but fails to achieve the optimal result neither suppress the NC. Although the approach implemented the usual limits on phase currents in the inner current control, this does not explicitly limit the NC. It is therefore possible for the NC current to exceed the ST current limit leading to overcurrent damage. Although there is a clear limit to the ability of the ST to reduce the NC if the voltage unbalance is to be maintained with the 2% (over 95% of the time) limit imposed by the standards, it remains the possibility to exceed this limit in exceptional circumstances (for 5% of the time). This requires a more advanced approach to NC minimization control which is closed loop and ensures NC current limitation in extreme situations. Therefore, the contribution of this paper is to propose a new optimal NC current suppression and limitation technique to achieve these aims. The proposed method consists of only algebraic equations which can be solved with relatively small computation effort so that it suitable for running in real time with a small sampling time.

The paper is structured as follows: Section II introduces the ST with 4-leg LV DC/AC inverter fed 3-phase 4-wire distribution system. Section III reviews the NC elimination control strategies. The NC optimal control and suppression control strategy are proposed in Section IV and Section V respectively. Section VI provides the experimental validation and Section VII presents the performance, from simulation, when applied in a 350 kVA, 400 V distribution network with unbalanced loads. Section VIII draws the conclusion of this paper.

II Smart Transformer-fed Distribution System

The basic configuration of a 3-stage ST consists of MV AC/DC rectifier, MVDC/LVDC converter with a medium frequency transformer and LVDC/AC inverter as shown in Fig.1. The main advantage of this configuration is that the voltage in the primary and secondary side of the ST is fully decoupled and can be regulated independently. Since the emphasis in this work is to reduce the NC in the LVAC, the control is implemented in the LV inverter, and thus, the work focuses on ST LV side inverter only.

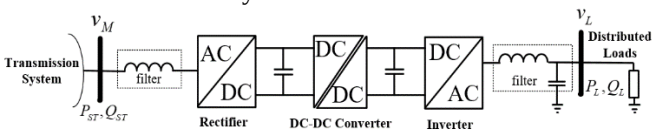

Fig. 1. Basic configuration of three-stage ST

Since the distribution system is 3-phase 4-wire, there are two methods which can be used to connect to such a system using the 3 phase LV inverter in the ST. One approach would be to connect the neutral line to the mid-point of DC capacitors. However, excessive NC would adversely affect the lifetime and reliability of the capacitors. Another method uses the 4-leg inverter (see Fig. 2), where the fourth leg connects to the neutral line. The additional leg can not only provide the path for the NC, but it also allows each phase-to-neutral to become independent. This gives greater freedom for the distribution system voltage regulation. Thus, the voltage can be purposely adjusted to be unbalanced in order to optimize and suppress the excessive NC. The control of the 4-leg inverter contains separate regulation on positive-, negative- and zero-sequence components based on the synchronous dq frame. Therefore, the analysis and the proposed control is based on the application of sequence components, pn0. Fig. 2 shows a simplified diagram of the 4 leg inverter, with LC filter, feeding 3-phase, unbalanced loads, Z_a, Z_b, Z_c, which will be used to illustrate the development of the control approach.

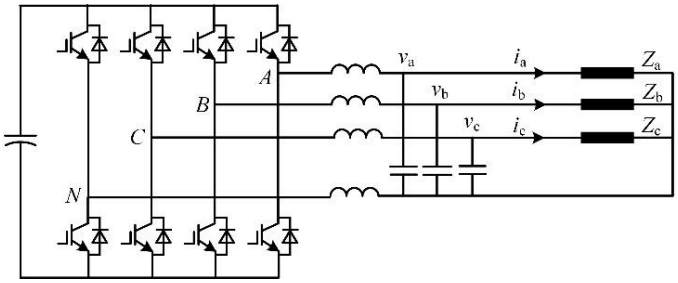

Fig. 2. Topology of 3-phase 4-leg inverter

Based on the definition of sequence components, three-phase PCC voltage V_{abc} equation can be expressed as,

$$\begin{bmatrix} V_p \\ V_n \\ V_0 \end{bmatrix} = \frac{1}{3}\begin{bmatrix} 1 & a & a^2 \\ 1 & a^2 & a \\ 1 & 1 & 1 \end{bmatrix}\begin{bmatrix} Z_a & Z_{ne} & Z_{ne} \\ Z_{ne} & Z_b & Z_{ne} \\ Z_{ne} & Z_{ne} & Z_c \end{bmatrix}\begin{bmatrix} 1 & 1 & 1 \\ a^2 & a & 1 \\ a & a^2 & 1 \end{bmatrix}\begin{bmatrix} I_p \\ I_n \\ I_0 \end{bmatrix} \quad (1)$$

where subscripts "*p*" "*n*" and "*o*" represent the positive-, negative- and zero-sequence component, respectively; subscripts "*a*" "*b*" "*c*" and "*ne*" distinguish the variables in phase-a, -b, -c and neutral; *V*, *I* and *Z* are the voltage, current and impedance respectively; *a* is the operator equalling to $1\angle 120°$.

Assuming that the neutral impedance is small enough to be negligible compared to loads, then by assuming Z_{ne}=0, (1) can be simplified as,

$$\begin{bmatrix} V_p \\ V_n \\ V_0 \end{bmatrix} = \frac{1}{3} M \begin{bmatrix} I_p \\ I_n \\ I_0 \end{bmatrix} \quad (2)$$

where

$$M = \begin{bmatrix} Z_a + Z_b + Z_c & Z_a + a^2 Z_b + a Z_c & Z_a + a Z_b + a^2 Z_c \\ Z_a + a Z_b + a^2 Z_c & Z_a + Z_b + Z_c & Z_a + a^2 Z_b + a Z_c \\ Z_a + a^2 Z_b + a Z_c & Z_a + a Z_b + a^2 Z_c & Z_a + Z_b + Z_c \end{bmatrix}$$

When the 3-phase system is balanced, V_p is equal to the rated value, while V_n, V_0, I_0 and I_n are equal to 0; otherwise, the system has a certain NC, i.e. $I_0 \neq 0$.

III Neutral Current Elimination Control

A Neutral Current Elimination Control

The NC elimination control which has been previously proposed in [31], had the objective of eliminating the NC. It proposed to set the voltage so as to compel the zero-sequence current to be 0, while keeping the positive and negative-sequence currents fixed, i.e. $I_0^{'} = 0, I_p^{'} = I_p$ and $I_n^{'} = I_n$, where $I_p^{'}, I_n^{'}$ and $I_0^{'}$ are the output sequence currents after application of the NC elimination control. By substituting these currents into (2), the required voltage can be obtained as,

$$\begin{bmatrix} V_p^{'} \\ V_n^{'} \\ V_0^{'} \end{bmatrix} = \frac{1}{3} \begin{bmatrix} Z_a + Z_b + Z_c & Z_a + a^2 Z_b + a Z_c \\ Z_a + a Z_b + a^2 Z_c & Z_a + Z_b + Z_c \\ Z_a + a^2 Z_b + a Z_c & Z_a + a Z_b + a^2 Z_c \end{bmatrix} \begin{bmatrix} I_p \\ I_n \end{bmatrix} \quad (3)$$

The corresponding abc voltages can be obtained as,

$$\begin{bmatrix} V_a^{'} \\ V_b^{'} \\ V_c^{'} \end{bmatrix} = \begin{bmatrix} 1 & 1 & 1 \\ a^2 & a & 1 \\ a & a^2 & 1 \end{bmatrix} \begin{bmatrix} V_p^{'} \\ V_n^{'} \\ V_0^{'} \end{bmatrix} = \begin{bmatrix} Z_a I_p + Z_a I_n \\ a^2 Z_b I_p + a Z_b I_n \\ a Z_c I_p + a^2 Z_c I_n \end{bmatrix} \quad (4)$$

Equation (4) shows that the required reference voltages can be calculated directly from the measured positive and negative sequence currents. Consequently, the resulting 3-phase output currents can be expressed as,

$$\begin{bmatrix} I_a^{'} \\ I_b^{'} \\ I_c^{'} \end{bmatrix} = \begin{bmatrix} V_a^{'} / Z_a \\ V_b^{'} / Z_b \\ V_c^{'} / Z_c \end{bmatrix} = \begin{bmatrix} I_p + I_n \\ a^2 I_p + a I_n \\ a I_p + a^2 I_n \end{bmatrix} \quad (5)$$

Then the NC $I_{ne}^{'}$ would be,

$$I_{ne}^{'} = I_a^{'} + I_b^{'} + I_c^{'} = (1 + a + a^2) I_p + (1 + a + a^2) I_n = 0 \quad (6)$$

In this way the NC could be eliminated by setting the zero-sequence current as 0 and using the original positive-, negative-sequence current.

B Voltage Unbalanced Requirement

In the real distribution systems, the phase angle and amplitude of voltage cannot be significantly varied, since a dramatically unbalanced output voltage has significant negative impacts on loads, such as induction machines. Consequently, standards such as EN50160 state that the unbalanced voltage degree in the distribution system, should be below 2% for 95% of the time [29]. Because the NC elimination control changes both voltage amplitude and phase, the estimation of voltage unbalance degree should consider amplitude and phase respectively under the following measures. According to the definitions in [32], the unbalanced voltage factor (UBF) and phase voltage unbalance degree PVUR can be expressed as,

$$\mathrm{PVUR} = \frac{|V_{max}| - |V_{min}|}{|V_{avg}|} \times 100\% \quad (7)$$

$$\mathrm{UBF} = \left| \frac{V_n}{V_p} \right| \times 100\% \quad (8)$$

where $|V_{max}|$, $|V_{min}|$, $|V_{avg}|$ are the maximum, minimum, average value of the amplitude of 3-phase output voltage respectively. Based on the comparison and analysis of the UBF and PVUR in a distribution system, it is suggested that both PVUR and UBF should be below 2% for the stable operation in the distribution system [33].

IV Neutral Current Minimization Control

The objective of NC reduction control is to reduce the NC while still satisfying the constraints of both PVUR and UBF. In other words, the work minimizes the NC, but because of the limited voltage operation required from the EN 50160 standard, the NC may not be completely eliminated, especially under the dramatic unbalanced situation. NC can be directly reduced by regulating and reducing only zero-sequence current $I_0^{'}$, while other components are remain constant, i.e. $I_p^{'} = I_p$ and $I_n^{'} = I_n$. When further reduction of the zero-sequence component requires a voltage unbalance greater than the limit, further NC reduction can be achieved by regulation of the negative sequence current component $I_n^{''}$, which can provide additional reduction on the zero-sequence current $I_0^{''}$. We use $'$ and $''$ to distinguish the NC under zero-sequence regulation only and the NC under further negative-sequence regulation, respectively.

A Zero-sequence Control

In the NC reduction control, the following constraints are defined, i) the controlled zero-sequence current is $I_0^{'}$, and $0 \leq |I_0^{'}| < |I_0|$; ii) the positive- and negative-sequence currents are fixed, i.e. $I_p^{'} = I_p$ and $I_n^{'} = I_n$; iii) the average voltage is equal to the rated value, i.e. $|V_{avg}| = |V_{rate}|$. Based on these constraints, (7) can be expressed as,

$$\max(|V_a|, |V_b|, |V_c|) - min(|V_a|, |V_b|, |V_c|) \leq 0.02 |V_{rate}| \quad (9)$$

Substituting the above conditions into (2) and transforming back to the three-phase stationary reference frame gives,

$$\begin{bmatrix} V_a^{'} \\ V_b^{'} \\ V_c^{'} \end{bmatrix} = \begin{bmatrix} Z_a I_p + Z_a I_n + Z_a I_0^{'} \\ a^2 Z_b I_p + a Z_b I_n + Z_b I_0^{'} \\ a Z_c I_p + a^2 Z_c I_n + Z_c I_0^{'} \end{bmatrix} \quad (10)$$

Based on (10), the absolute value of voltage is determined by the load impedance. For simplification of the presentation of the analysis, it is assumed that the relationship among load impedance is: $Z_a \leq Z_b \leq Z_c$. Then, $|V_c^{'}|$ is the maximum

value while $|V_a^{'}|$ is the minimum value, and (9) can be expressed as:

$$|V_c^{'}| - |V_a^{'}| \le 0.02V_{rate} \quad (11)$$

Since phase-c leads phase-a by 120°, by substituting (10) into (11) yields,

$$V_c^{'}a^2 - V_a^{'} = Z_cI_p + aZ_cI_n + a^2Z_cI_0^{'} - (Z_aI_p + Z_aI_n + Z_aI_0^{'}) = (Z_c - Z_a)I_p + (aZ_c - Z_a)I_n + (a^2Z_c - Z_a)I_0^{'} \quad (12)$$

In the balanced voltage case,

$$|V_c| - |V_a| = V_ca^2 - V_a = (Z_c - Z_a)I_p + (aZ_c - Z_a)I_n + (a^2Z_c - Z_a)I_0 = 0 \quad (13)$$

Hence:

$$(Z_c - Z_a)I_p + (aZ_c - Z_a)I_n = -(a^2Z_c - Z_a)I_0 \quad (14)$$

Substituting (14) into (12) gives:

$$V_c^{'}a^2 - V_a^{'} = -(a^2Z_c - Z_a)I_0 + (a^2Z_c - Z_a)I_0^{'} = (a^2Z_c - Z_a)(I_0^{'} - I_0) \le 0.02V_{rate} \quad (15)$$

For $I_0^{'} - I_0 \le 0$ and $a^2Z_c - Z_a = -Z_a - \frac{1}{2}Z_c + j\frac{\sqrt{3}}{2}Z_c < 0$, then the resulting NC when the voltages still satisfies the PVUR constraints, can be expressed as :

$$I_0^{'} = I_0 + \frac{0.02V_{rate}}{(a^2Z_c - Z_a)} \quad (16)$$

Note, the obtained $|I_0^{'}| \in [0, |I_0|)$. When the load is balanced, (16) would compute a negative value. In this situation, the NC $I_0^{'}$ should set to 0. Otherwise, it would make the voltage unbalanced and give rise to the NC.

B Negative-sequence Control

When (16) is satisfied, PVUR meets the limitation. However, the PVUR (7) does not have any requirement on phase angle and thus we could change the negative-sequence current $I_n^{''}$, in order to further reduce the NC to $I_0^{''}$ until the UBF condition (17) is broken.

$$|V_n^{'}| \le 0.02V_{rate} \quad (17)$$

In this case, the voltage would be changed to:

$$\begin{bmatrix} V_a^{''} \\ V_b^{''} \\ V_c^{''} \end{bmatrix} = \begin{bmatrix} Z_aI_p + Z_aI_n^{''} + Z_aI_0^{''} \\ a^2Z_bI_p + aZ_bI_n^{''} + Z_bI_0^{''} \\ aZ_cI_p + a^2Z_cI_n^{''} + Z_cI_0^{''} \end{bmatrix} \quad (18)$$

By substituting (18) into (7) and according to (12)-(16), similarly, it can be obtained that,

$$V_c^{''}a^2 - V_a^{''} = (aZ_c - Z_a)(I_n^{''} - I_n) + (a^2Z_c - Z_a)(I_0^{''} - I_0) \le 0.02V_{rate} \quad (19)$$

Equation (19) is used to constrain the PVUR. Now, we consider UBF condition, for which the negative-sequence voltage magnitude can be expressed as (20) in the balanced condition.

$$|V_n| = \frac{(Z_a + aZ_b + a^2Z_c)I_p}{3} + \frac{(Z_a + Z_b + Z_c)I_n}{3} + \frac{(Z_a + a^2Z_b + aZ_c)I_0}{3} = 0 \quad (20)$$

Assuming the positive-sequence voltage remains at rated after voltage regulation, i.e. $|V_p^{''}| = V_{rate}$ and as the positive-sequence control does not change, i.e. $I_p^{''} = I_p$, substituting these two conditions along with (20) into (8) gives:

$$|V_n^{''}| = (Z_a + Z_b + Z_c)(I_n^{''} - I_n) + (Z_a + a^2Z_b + aZ_c)(I_0^{''} - I_0) \le 0.06V_{rate} \quad (21)$$

Assuming the further reduced NC is ΔI_0, i.e. $I_0^{''} = I_0^{'} - \Delta I_0$, substituting into (19) gives that,

$$(aZ_c - Z_a)(I_n^{''} - I_n) = (a^2Z_c - Z_a)\Delta I_0 \quad (22)$$

and

$$I_n^{''} - I_n = \frac{(a^2Z_c - Z_a)\Delta I_0}{(aZ_c - Z_a)} \quad (23)$$

Substituting (20), (23) and $I_0^{''} = I_0^{'} - \Delta I_0$ into (19) obtains

$$\left[(Z_a + Z_b + Z_c)\frac{(a^2Z_c - Z_a)}{(aZ_c - Z_a)} - (Z_a + a^2Z_b + aZ_c)\right]\Delta I_0 \le 0.06V_{rate} - (Z_a + a^2Z_b + aZ_c)\frac{0.02V_{rate}}{(a^2Z_c - Z_a)} \quad (24)$$

For $Z_a \le Z_b \le Z_c$, $\mathrm{Re}(I_0) \ge \mathrm{Re}(I_0^{'}) \ge \mathrm{Re}(I_0^{''}) \ge 0$ and $\mathrm{Im}(I_0) \le \mathrm{Im}(I_0^{'}) \le \mathrm{Im}(I_0^{''}) \le 0$. The maximum ΔI_0 would be,

$$\Delta I_0 = \frac{0.06V_{rate} - (Z_a + a^2Z_b + aZ_c)\frac{0.02V_{rate}}{(a^2Z_c - Z_a)}}{(Z_a + Z_b + Z_c)\frac{(a^2Z_c - Z_a)}{(aZ_c - Z_a)} - (Z_a + a^2Z_b + aZ_c)} \quad (25)$$

Then the minimized zero-sequence (neutral) current is (26) and its corresponding negative-sequence current variation is (27).

$$I_0^{''} = \frac{0.02V_{rate}}{(a^2Z_c - Z_a)} + I_0 - \Delta I_0 \quad (26)$$

$$I_n^{''} = \frac{(a^2Z_c - Z_a)\Delta I_0}{(aZ_c - Z_a)} + I_n \quad (27)$$

Substituting (26) and (27) back to (18) could obtain the reference voltage for the minimal NC which satisfies the standard requirement. It should be noted that $|I_0^{'}| \in [0, |I_0|)$, and $|I_0^{''}| \in [0, |I_0^{'}|)$. If these conditions break, it means zero-sequence crosses the zero NC operating point and reduces to be opposite sign with higher magnitude, thus, set $I_0^{''} = 0$ and $I_n^{''} = I_n$ to fully eliminate NC.

C Initialization

Implementation of the proposed control in (18) requires the following information, the total load impedance in each phase viewed from the ST terminal Z_a, Z_b, Z_c and the initial currents I_n, I_p, I_0.

Although the proposed method only minimizes the NC on the ST connected line, according to Kirchhoff's Current Law (KCL) and if the distributed load power factor is approaching to unity with small phase shift, the total NC reduction on the main branch must lead to NC reduction in other lines. Although the loads are distributed and stochastic, the real-time measurement in the ST can identify the load impedance via the measurement of voltage, current, real and reactive powers, as shown in (28). These two points will be verified later using the

dynamic load in the hardware test and network simulation. Note that the impedance measurement is only aimed at the measurement of fundamental impedance, by the relatively simple technique of taking suitably low pass filtered measurements of voltage, current, real and reactive powers. In general, the distribution grid impedance varies with time and includes harmonic components. The accurate measurement of grid impedance is an active area of research [34-36] and any of those methods could be substituted for the approach adopted here.

$$\begin{bmatrix} Z_a \\ Z_b \\ Z_c \end{bmatrix} = \begin{bmatrix} \frac{|V_a|}{|I_a|}(\cos(\tan^{-1}\frac{Q_a}{P_a}) + \sin(\tan^{-1}\frac{Q_a}{P_a})j) \\ \frac{|V_b|}{|I_b|}(\cos(\tan^{-1}\frac{Q_b}{P_b}) + \sin(\tan^{-1}\frac{Q_b}{P_b})j) \\ \frac{|V_c|}{|I_c|}(\cos(\tan^{-1}\frac{Q_c}{P_c}) + \sin(\tan^{-1}\frac{Q_c}{P_c})j) \end{bmatrix} \quad (28)$$

The control requires the positive-, negative- and zero sequence current in the balanced voltage situation. Assuming phase-a voltage is the reference at rated value (V_{rate}), then:

$$\begin{bmatrix} I_p \\ I_n \\ I_0 \end{bmatrix} = \frac{1}{3}\begin{bmatrix} \frac{V_a}{Z_a} + a\frac{V_b}{Z_b} + a^2\frac{V_c}{Z_c} \\ \frac{V_a}{Z_a} + a^2\frac{V_b}{Z_b} + a\frac{V_c}{Z_c} \\ \frac{V_a}{Z_a} + \frac{V_b}{Z_b} + \frac{V_c}{Z_c} \end{bmatrix} = \frac{1}{3}\begin{bmatrix} \frac{V_{rate}}{Z_a} + \frac{V_{rate}}{Z_b} + \frac{V_{rate}}{Z_c} \\ \frac{V_{rate}}{Z_a} + a\frac{V_{rate}}{Z_b} + a^2\frac{V_{rate}}{Z_c} \\ \frac{V_{rate}}{Z_a} + a^2\frac{V_{rate}}{Z_b} + a\frac{V_{rate}}{Z_c} \end{bmatrix} \quad (29)$$

Through (28) and (29) the load impedance and initial sequence current can be dynamically computed. Substituting these results into (26) and (27) gives the required targets, zero- and negative-sequence current respectively. Then, the confirmed sequence currents (I_p, I_n'', I_0'') in (18) can be used to compute the reference voltage (V_a'', V_b'', V_c'') . The NC minimization control algorithm (16, 25-29) are algebraic equations, so that it can dynamically work on real-time.

V Neutral Current Suppression Control

The NC minimization control can be used in normal operation to reduce the NC and save the losses. However, in some extreme cases, the NC may be greater than the ST current limit. In this case, the NC has to be limited to avoid overcurrent damage or ST disconnection. Particularly, in some distribution systems, the NC is required to be limited to a maximum percentage of its phase current [37], e.g. maximum of 35.6% of phase in hospitals, 55% in public buildings and around 20% in the central telephone exchange [38]. EN 50160 [29] allows temporarily exceeding the voltage unbalance degree for 5% of the time. Thus, the ST could further suppress the NC by the means of purposely increasing the voltage unbalance degree beyond the limit. The standard voltage unbalance degree of 2%, is represented in (16, 25, 26) of the NC minimization control algorithm. An additional control algorithm is proposed in this section to link the voltage unbalance degree and the NC limits in order to supress the NC meanwhile optimizing this temporal voltage unbalance degree.

A PVUR-based Neutral Current Suppression

Since the negative-sequence voltage has high impacts on three-phase machines, the increase of PVUR is studied first. Assuming the PVUR=m when the suppression control is enabled, the maximum zero-sequence current would be $|I_{0,max}| = \frac{1}{3}|I_{ne,max}|$. Substituting these conditions into (25), (26) obtains the change in zero-sequence current, which should be less than $|I_{0,max}|$.

$$\Delta I_0 = \frac{0.06V_{rate} - (Z_a + a^2Z_b + aZ_c)\frac{mV_{rated}}{(a^2Z_c - Z_a)}}{(Z_a + Z_b + Z_c)\frac{(a^2Z_c - Z_a)}{(aZ_c - Z_a)} - (Z_a + a^2Z_b + aZ_c)} \quad (30)$$

$$I_0'' = \frac{mV_{rated}}{(a^2Z_c - Z_a)} + I_0 - \Delta I_0 \quad (31)$$

The objective is to ensure $|I_0''| \le |I_{0,max}|$ and meanwhile find the minimum value of m. By substituting (30) into (31) gives,

$$I_0'' = Am + B + I_0 \quad (32)$$

where $A = \frac{V_{rated}}{(a^2Z_c - Z_a)} + \frac{(Z_a + a^2Z_b + aZ_c)\frac{V_{rated}}{(a^2Z_c - Z_a)}}{(Z_a + Z_b + Z_c)\frac{(a^2Z_c - Z_a)}{(aZ_c - Z_a)} - (Z_a + a^2Z_b + aZ_c)}$

$$B = \frac{0.06V_{rate}}{(Z_a + Z_b + Z_c)\frac{(a^2Z_c - Z_a)}{(aZ_c - Z_a)} - (Z_a + a^2Z_b + aZ_c)}$$

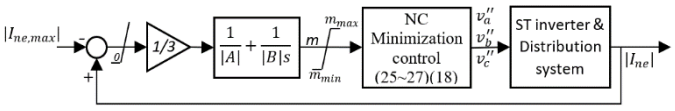

Fig. 3. PVUR Neutral Current Suppression Control Scheme

It indicates that the NC can be dynamically regulated by computing m in (32) with a PI controller as shown in Fig. 3. Based on (32), the proportional and integral gain is set as 1/|A| and 1/|B|, respectively. However, in reality, the load impedance Z_a, Z_b, Z_c changes randomly. To avoid the use of an adaptive PI controller, the value of |A| and |B| could be obtained by setting the load impedance equal to the rated power. For example, in 350 kVA, 400V distribution network, $Z_a = Z_b = Z_c = \frac{(400/\sqrt{3})^2}{350\times10^3/3}\Omega$ for |A| and |B| calculation. In addition, standard EN50160 also constraints the voltage variation within ±10%, i.e. $m_{max} = 0.1$. The lower saturation "0" at the input comparator makes the normal operation at $m_{min} = 0.02$.

B UBF-based Neutral Current Suppression

It is possible that PVUR-based NC suppression control becomes saturated, while the NC is still excessive. In this case, the UBF could also be temporarily increased to help with further decrease in NC. The increase in negative-sequence voltage would shift the voltage phase, which also benefits the reduction of harmonic NC caused by the triple-N harmonics, as the unbalance in voltage phase results in some degree of triple-N harmonic cancelation.

Assumed the UBF=n then rewrites (32) as,

$$I_0'' = Cn + D + I_0 \quad (33)$$

where $C = \frac{3V_{rate}}{(Z_a + Z_b + Z_c)\frac{(a^2Z_c - Z_a)}{(aZ_c - Z_a)} - (Z_a + a^2Z_b + aZ_c)}$

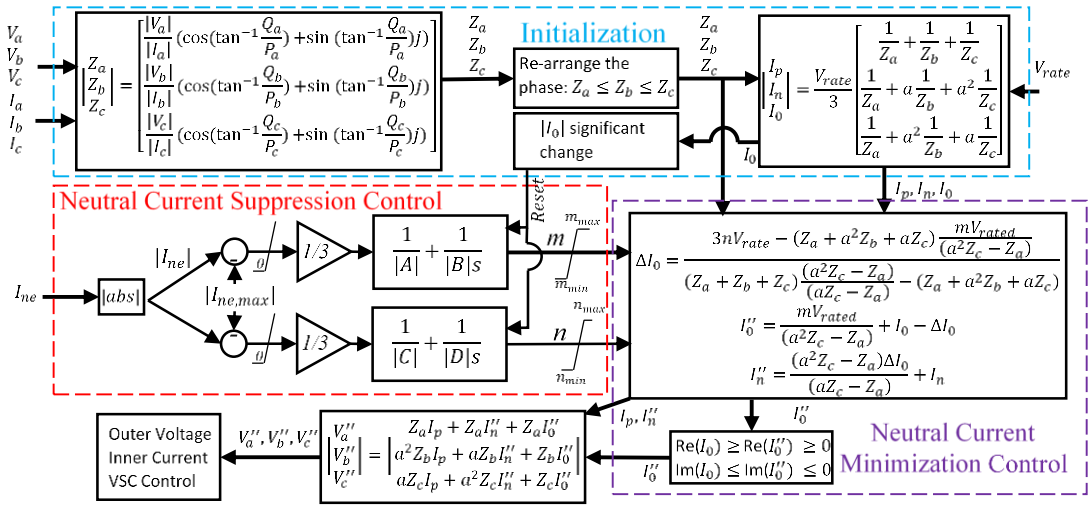

Fig. 5. Neutral Current Optimization Control Scheme

$$D = \frac{m_{max}V_{rated}}{(a^2Z_c - Z_a)} + \frac{(Z_a + a^2Z_b + aZ_c)\frac{m_{max}V_{rated}}{(a^2Z_c - Z_a)}}{(Z_a + Z_b + Z_c)\frac{(a^2Z_c - Z_a)}{(aZ_c - Z_a)} - (Z_a + a^2Z_b + aZ_c)}$$

Similar to Fig. 3, the UBF-based NC suppression control scheme is shown in Fig.4, where $n_{min} = 0.02$, $n_{max} = 0.1$.

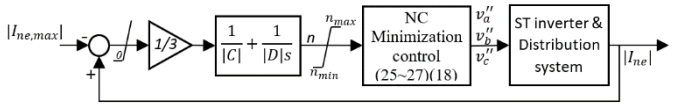

Fig. 4. UBF Neutral Current Suppression Control Scheme

C Overall Control Design

Fig. 5 shows the overall control design. The NC is measured and feedback to the NC suppression control. The NC suppression control provides the reference for the unbalance degree *m* and *n*, which is provided to the NC minimization control. This complete closed-loop control scheme is referred to as NC optimization control. The NC suppression control is automatically enabled only when the NC exceeds its limitation, otherwise the reference voltage unbalance degrees are set at 2% and the NC is minimized by the minimization control. The overall NC optimization control algorithm generates the reference sequence-currents and further obtains the reference voltages provides to the outer voltage, inner current control of the 4-leg voltage source converter. In order to automatically reset voltage unbalance degree back to 2%, the NC suppression control resets when the NC undergoes a significant change, e.g. 10%. Note that the use of the UBF based neutral current suppression control to temporarily exceed the limits imposed by the standard is envisaged as an emergency reaction which could be used to protect the ST from overcurrent.

VI Hardware Validation

In order to validate the proposed control approaches, a 2 kVA downscaled prototype of a 3-phase 4-leg inverter has been implemented with the hardware-in-the-loop experiment via Opal-RT, where the DC voltage is supplied via a rectifier connecting to the grid, the 4-leg inverter feeds to the loads via a 2 Ω emulated transmission line. The loads are varied and will be given in each test. The NC control scheme in Fig. 5 is implemented in the OP5600 Series OPAL-RT simulators. The OPAL-RT samples the voltage and current, and then after running the inverter controls, generates the firing pulses to drive the 4-leg inverter. The hardware set-up is shown in Fig. 6 as well as the set-up parameters are given in Table I. The NC minimization and NC suppression control are validated, respectively.

TABLE I
ELECTRICAL AND CONTROL PARAMETERS OF SIMULATION

Parameters	Symbols	Values
Rated power (kVA)	S	2
Switching frequency(kHz)	f_s	3
LC Filter capacitor(μF)	C_f	80
LC Filter inductor(mH)	L_f	65
DC bus voltage (V)	U_{dc}	500
Output AC voltage(V)	U_m	220
Line impedance (Ω)		2
Parameters of PI controllers		
Proportional gain of current PI	k_{p_c}	0.54
Integral gain of current PI	k_{i_c}	12
Proportional gain of voltage PI	k_{p_v}	134
Integral gain of voltage PI	k_{i_v}	584

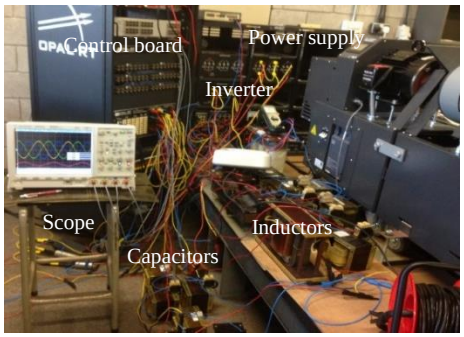

Fig. 6. Hardware-in-the-loop experiment set-up.

Note, the switch between the proposed control and balanced voltage control causes a transient peak in the PVUR and UBF in the test, e.g. in Fig. 8 at 2 s, Fig. 9 at 1 s, Fig. 10 at 1 s and 3 s, and Fig. 11 at 1 s and 3 s. However, if the inverter remains working on the proposed NC optimal method, no overshoot occurred in the PVUR and UBF even when the load suddenly changes as shown in Fig. 8 at 3 s and 4 s, Fig. 9 at 2 s and 3 s, Fig. 10 at 2 s and Fig. 11 at 2 s. In practice the proposed control would run continuously, and such transient spikes

would not be present. The switch between balanced voltage control and NC control is used in the test only to highlight the difference.

A Neutral Current Optimization Control Validation: Neutral Current Minimization Control

To validate the minimization NC control in the test, the three-phase load unbalance degree is dynamically changed: the initial value of load unbalanced degree is 9.4% (48/48/63Ω+27mH/phase), and then increases to 47% (63/63/98Ω+27mH/phase) at 3s and 71.8% (48/63/98Ω +27mH/phase) at 4s. Considering the line impedance is 2 Ω in this test, the theoretical impedance in each phase at each time is following:

1.5-3 s: *A*: 50.7∠0.167Ω; B: 50.7∠0.167Ω; C: 65.5∠0.13Ω.

3-4 s: A: 65.5∠0.13Ω ; B: 65.5∠0.13Ω; C: 100.4∠0.085Ω

4-5 s: *A*: 50.7∠0.167Ω; B: 65.5∠0.13Ω; C: 100.4∠0.085Ω

Fig. 7 shows the test results as obtained from the measurement technique which can be seen to be quite close the actual value as above. The impedance amplitude can be computed within 0.1 s, which is delayed by the RMS calculation. While the impedance angle computation has a 0.5 s delay, this is because of the low pass filter used to measure the power in fundamental component, but this does not affect the control as shown latter in Fig. 8.

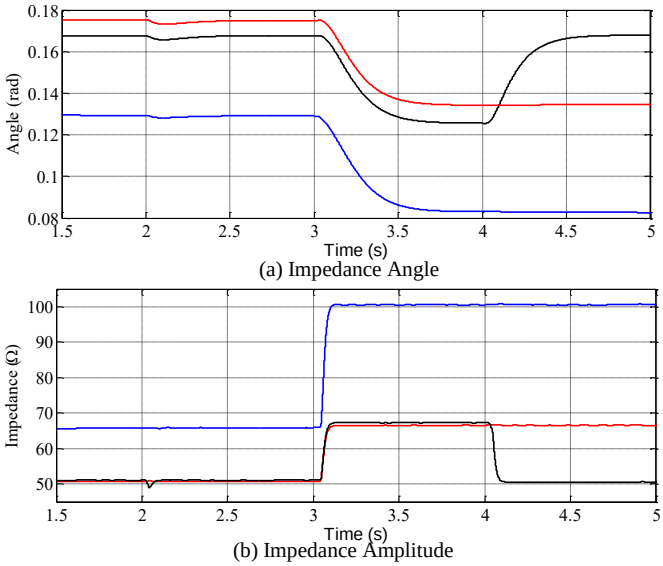

Fig. 7. Experimental results of impedance measurement (a) angle (b) amplitude, 1.5-3 s, 48/48/63Ω+27 mH/phase; 3-4s 63/63/98Ω+27mH/phase, 4-5s 48/63/98Ω+27mH/phase.

Fig. 8 presents the results under different control, including the balanced voltage (blue), proposed NC minimization control (red) and elimination control (black). From 1.5s to 2s, only the balanced voltage control is adopted and at 2s the NC minimization control and NC elimination control is enabled.

The increase of the load unbalanced degree leads to the NC increase under the balanced voltage control as shown in Fig.8(a) (blue trace). The NC elimination control can reduce NC almost to zero (black trace), but this requires a large unbalanced voltage degree as can be seen from the PVUR in Fig.8 (b) and the UBF in Fig.8 (c). This action significantly violates the limits for the voltage unbalance degree, especially the PVUR. In contrast, the NC minimization control minimizes the NC meanwhile ensuring that the voltage unbalance degree is within 2%.

In theory both the proposed method and the neutral current elimination control should also reduce ripple on the ST DC link due to the unbalance, however in practice this effect is small. It can be seen from Fig. 8 (d) that the neutral current controls, including both proposed method and NC elimination method, has no influence on the DC side voltage compared with the balanced voltage control. The main influence on the DC voltage comes from a significant power change or specifically the loading change.

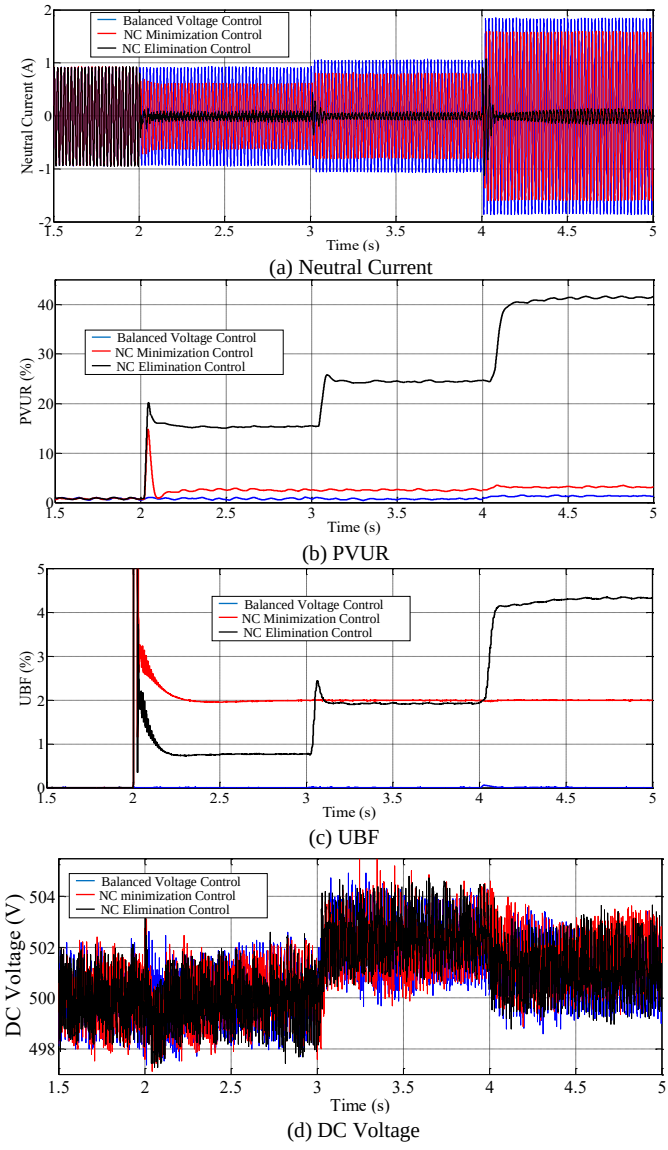

Fig. 8. Experimental results of (a) Neutral Current (b) PVUR, (c) UBF, (d) DC Voltage (1.5-2 s balanced voltage control; 2-5 s the tested control activated, 1.5-3 s 48/48/63Ω+27 mH/phase; 3-4s 63/63/98Ω+27mH/phase, 4-5s 48/63/98Ω+27mH/phase).

B Neutral Current Optimization Control Validation: Neutral Current Suppression Control

The NC suppression control includes the calculation of both PVUR- and UBF-based references, and in order to highlight the working of the control, so that these two parts are tested separately. Fig. 9 presents the results from the NC suppression control. In this case, the load is static at 48/63/98Ω+27mH/phase with 71.8% unbalanced degree. At 1s, the NC optimization control (as tested in the previous section) with *m*=0.02 and *n*=0.02 is activated; the PVUR- and UBF-based suppression parts are enabled at 2s and 3s separately. For the sake of the test it is assumed that the maximum allowable NC, $|I_{ne,max}|$ is set as 1A and reduction of the NC below this limit cannot be achieved by the control with m=0.02 and n=0.02 as indicated by the portion of the trace between 1s and 2 s in Fig. 9(a). Under these conditions the NC suppression control activates and the voltage unbalance degree, *m* and *n*, (PVUR and UBF) are temporarily increased to help keep the NC within the limit. For the test, the PVUR and UBF control parts are decoupled, i.e. the UBF (Fig.9 (b)) is constant when the PVUR control part is active and vice versa. As can be seen in this case, the increase in PVUR alone up to 10% (between 2s and 3s) is not sufficient to reduce the neutral current and the increase in UBF to 5% is required.

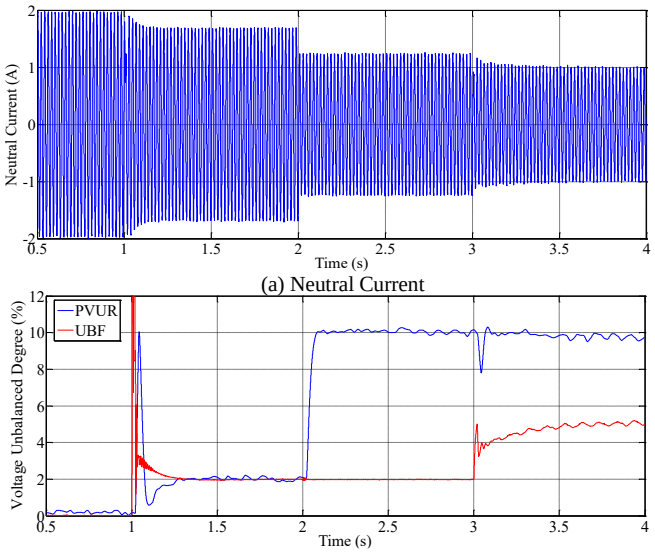

(a) Neutral Current

(b) Voltage Unbalanced Degree

Fig. 9. Experimental results of (a) NC and (b) voltage unbalance degree (0.5-1s balanced voltage control; 1-2s NC minimization control; 2-3s PVUR-based suppression control; 3-4s UBF-based NC suppression control with load 48/63/98 Ω+27mH/phase)

Fig. 10 shows test results from load step changes from 48/63/98Ω+27mH/phase to 63/63/98Ω+27mH/phase at 2s to validate the performances of the NC suppression control under the dynamic load situation. The control approach follows Fig. 5, including of the PVUR and UBF-based NC suppression control and NC minimization control, which are enabled simultaneously from 1 s to 3 s and then back to the balanced voltage control after 3 s. It can be seen that the activation of the NC optimization control can immediately supress the NC from 1 s. When the load unbalanced degree reduces, the control can automatically tune the voltage unbalance degree back to 2% at 2 s. Note in Fig. 10 around 1.5 s, the voltage unbalanced degree for PVUR and UBF are identical to that in Fig. 9 at 4 s due to the same loading conditions. This helps verify that the NC suppression control for PVUR and UBF are independent, and their simultaneous action causes no problem.

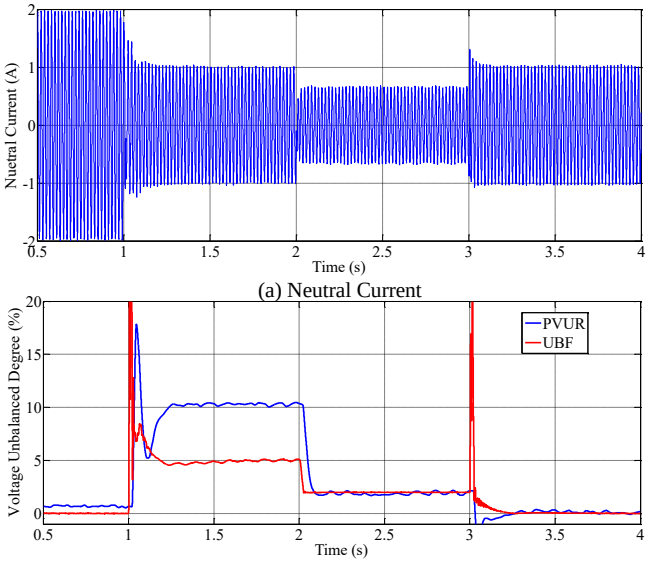

(a) Neutral Current

(b) Voltage Unbalanced Degree

Fig. 10. Experimental results of (a) NC, and (b) voltage unbalance degree; (0.5-1s balanced voltage control; 1-3s NC suppression control; 3-4s balanced voltage control. Load step change from 48/63/98 Ω+27mH/phase to 63/63/98 Ω+27mH/phase at 2s)

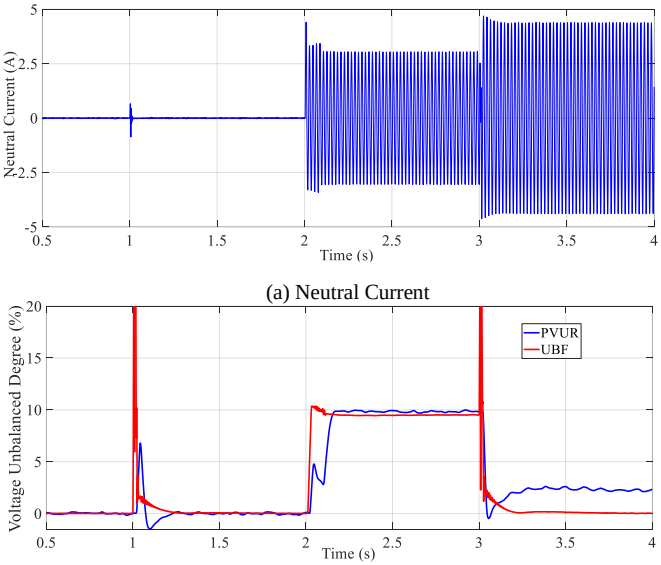

(a) Neutral Current

(b) Voltage Unbalanced Degree

Fig. 11. Experimental results of (a) NC and (b) voltage unbalance degree (0.5-1s and 3-4s balanced voltage control; 1-3s NC optimization control with balanced load 48Ω+27mH/phase during 0.5-2 s; phase C open-short fault during 2-4s)

C Open-short Fault

The proposed NC optimization control has also been verified under an asymmetric open fault test, where the load starts from a balanced load, 48Ω+27mH/phase and subsequently phase C is open at 2 s. To compare with the balanced voltage regulation,

the proposed control is enabled at 1 s and disabled at 3s. Fig. 11 presents the results and proves that the control maintains zero NC when the load is balanced and reduces the NC even in the case of the single phase open fault as much as is possible while keeping the voltage unbalanced degree below the maximum 10%.

VII Case Study

In order to further verify the practicability of the proposed NC optimization control strategies, the control is applied to an ST assumed to be feeding a 350 kVA, 400 V urban distribution network with 90 residential customers evenly distributed across three phases, i.e. 32, 26, and 32 customers in phase A, B and C respectively. The distribution network (in Fig. 12), based on ENWL distribution grid Feeder 3 in the Manchester area, has 90 residential customers evenly distributed across three phases, with 32, 26, and 32 customers in phase A, B and C respectively. The load is modelled as an exponential load, i.e. $P = P_{rated}(\frac{V}{V_{rated}})^{\alpha}, Q = Q_{rated}(\frac{V}{V_{rated}})^{\beta}$ with voltage coefficient $\alpha \in [0.5\ 1.5]$ $\beta \in [1\ 1.8]$ as detailed in Fig. 13 (b) [10], where P_{rated}/Q_{rated} is the rated power. The data for each customer is obtained by averaging the total power (see Fig. 13 (a)) in the corresponding phase and then randomizing between 90% to 110%. The power factor is randomized between 0.92 to 0.98. The distribution model was built in the software Matlab/Simulink running in real-time with the details in [39], with one-minute load data resolution scaled to one second in the simulation.

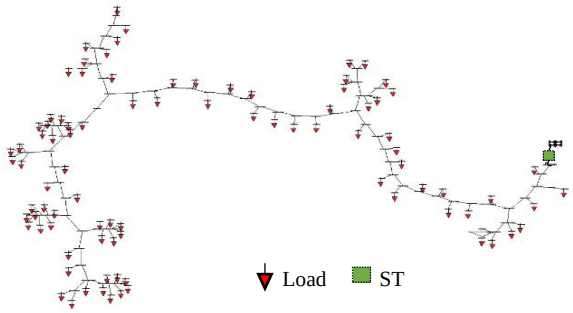

Fig. 12. ENWL Distribution grid in the Manchester with ST

Fig.14 (a) shows the NC results on the ST terminal under the proposed NC optimization control and the conventional balanced voltage control. Clearly, the NC optimization control can reduce the NC on average by 20% as shown in Fig.14 (b). Note, for some short durations when the load is lightly unbalanced, the NC can be totally eliminated in Fig. 14 (b). When the NC does not exceed its limiation (here set at 143 A), the control fulfils the EN50160 standard with 2% voltage unbalanced degree, while when the NC exceeds its limit, the unbalanced degree is temporarily increased in order to suppress the excessive NC below 143 A as shown in Fig.14(a) and (c). Fig.14 (d) and (e) show the zoomed-in results around 1080 s, when the NC is excessive. At 1085 s, the original NC (blue line) increased by 11.52% from 165 to 184A; which is over 10%, so that the NC suppression control is reset. This is why the NC shows a surge from 143 to 162 A even under the proposed control at this time. The dynamic of the proposed NC control has an associated time constant (due ot the PI control), and adjusts the allowable voltage unbalanced degree until the NC is below the limit. When the original NC reduces by 10% (blue line from 184 A to 165.6A at 1086s), the NC suppression control resets again, and due to the NC being within the limit, it maintains 2% voltage unbalanced degree.

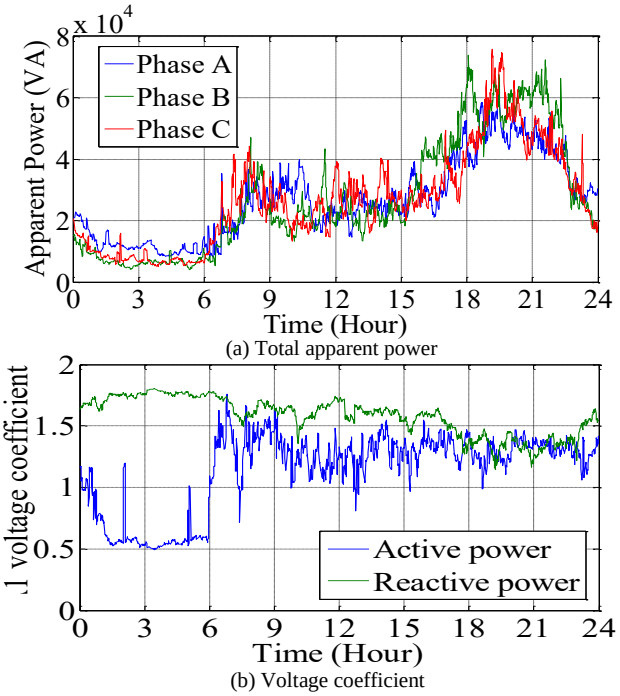

Fig. 13. One-day loading profile

Table II summaries the loss in the neutral lines. Since the control is applied to minimize the neutral current at the ST connection point, there is no doubt that the loss in this section of neutral line reduces by 25%. However, the section of neutral line carrying the full NC seen by the ST is relatively short and downstream lines are more significant as regards losses shown in Fig. 12. As expected, although the neutral current is only directly controlled in the ST connected line, it also has to reduce in the other lines. Therefore, the total downstream neutral line energy loss (over the course of 24 hours) is reduced from 17.83 kWh to 13.81 kWh, around 22.55% reduction. This verifies that the proposed NC optimization control can not only reduce the losses on the connected line but also in the downstream lines, thus benefiting to the whole distribution system.

TABLE II
DAILY NEUTRAL LINE LOSSES COMPARISON (KWH)

Line	Balanced voltage control	Proposed control	Losses reduction
ST connected line	0.20	0.15	25.00%
Total downstream lines	17.83	13.81	22.55%
Total lines	18.03	13.96	22.57%

VIII Conclusions

This paper proposes a practical neutral current optimization control suitable to be implemented in the Smart Transformer-

fed 3-phase 4-wire distribution system to minimize and suppress the neutral current optimally. Two constraints, voltage unbalanced degree and ST overcurrent, are both considered for the neutral current operation. When the NC is exceeds the ST capacity, a temporary higher voltage unbalance degree is applied to supress the NC within the ST current limit; otherwise, the control minimizes the NC under a maximum 2% voltage unbalance degree.

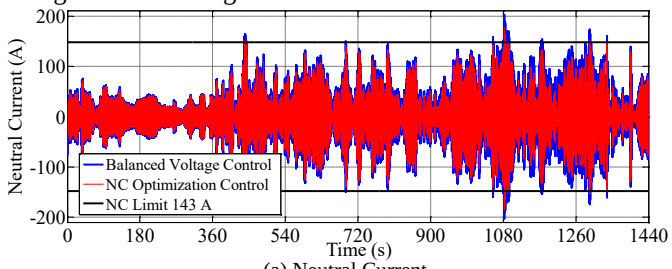

(a) Neutral Current

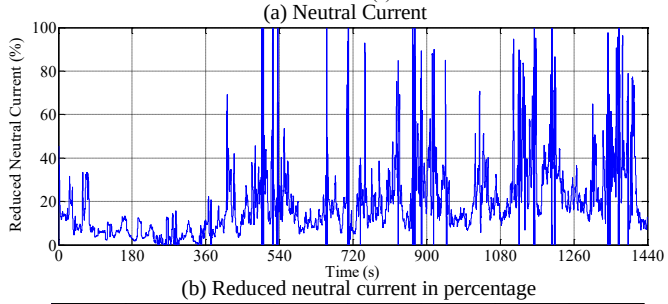

(b) Reduced neutral current in percentage

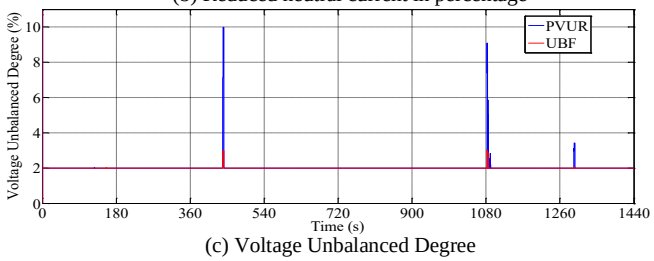

(c) Voltage Unbalanced Degree

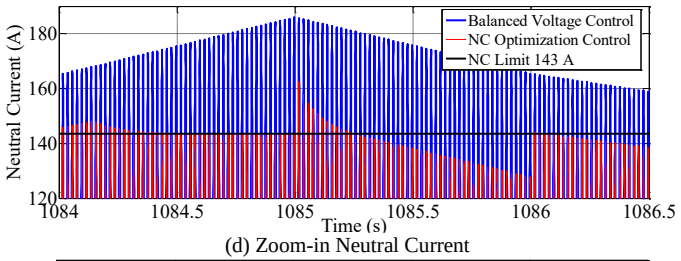

(d) Zoom-in Neutral Current

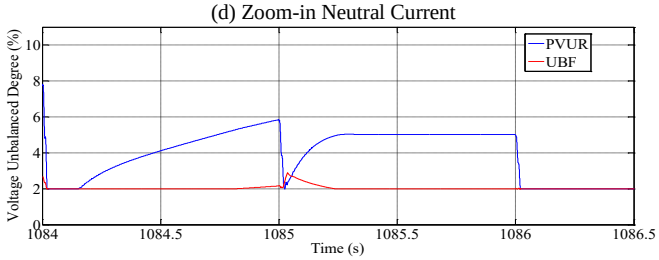

(e) Zoom-in Voltage Unbalanced Degree

Fig. 14. Distribution network simulation results of (a) neutral current, (b) reduced neutral current in percentage, (c) voltage unbalanced degree, (d) zoom-in neutral current and (e) zoom-in voltage unbalanced degree.

REFERENCES

[1] L. Ferreira Costa, G. De Carne, G. Buticchi and M. Liserre, "The Smart Transformer: A solid-state transformer tailored to provide ancillary services to the distribution grid," *IEEE Power Electron. Mag.*, vol. 4, no. 2, pp. 56-67, June 2017.

[2] She X, Burgos R, Wang G, et al. "Review of solid state transformer in the distribution system: From components to field application." *IEEE Energy Conversion Congress and Exposition (ECCE)*. IEEE, 4077–4084.

[3] R. Zhu, G. De Carne, F. Deng and M. Liserre, "Integration of Large Photovoltaic and Wind System by Means of Smart Transformer," in *IEEE Transactions on Industrial Electronics*, vol. 64, no. 11, pp. 8928-8938, Nov. 2017.

[4] X. Gao, F. Sossan, K. Christakou, M. Paolone and M. Liserre, "Concurrent Voltage Control and Dispatch of Active Distribution Networks by Means of Smart Transformer and Storage," *IEEE Transactions on Industrial Electronics*, vol. 65, no. 8, pp. 6657-6666, Aug. 2018

[5] C. Kumar, R. Zhu, G. Buticchi and M. Liserre, "Sizing and SOC Management of a Smart-Transformer-Based Energy Storage System," *IEEE Transactions on Industrial Electronics*, vol. 65, no. 8, pp. 67096718, Aug. 2018

[6] H. Hua, Y. Qin, C. Hao and J. Cao, "Stochastic Optimal Control for Energy Internet: A Bottom-Up Energy Management Approach," in *IEEE Transactions on Industrial Informatics*, vol. 15, no. 3, pp. 1788-1797, March 2019.

[7] A. Q. Huang, M. L. Crow, G. T. Heydt, J. P. Zheng, and S. J. Dale, "The future renewable electric energy delivery and management (FREEDM) system: The energy internet," *Proc. IEEE*, vol. 99, no. 1, pp. 133– 148, Jan. 2011

[8] G. De Carne, G. Buticchi, M. Liserre and C. Vournas, "Load Control Using Sensitivity Identification by Means of Smart Transformer," in *IEEE Transactions on Smart Grid*, vol. 9, no. 4, pp. 2606-2615, July 2018.

[9] G. De Carne, M. Liserre and C. Vournas, "On-Line Load Sensitivity Identification in LV Distribution Grids," in *IEEE Transactions on Power Systems*, vol. 32, no. 2, pp. 1570-1571, March 2017.

[10] J. Chen, C. O'Loughlin and T. O'Donnell, "Dynamic demand minimization using a smart transformer," *IECON 2017 - 43rd Annual Conference of the IEEE Industrial Electronics Society*, Beijing, 2017, pp. 4253-4259.

[11] J. Chen *et al.*, "Smart Transformer for the Provision of Coordinated Voltage and Frequency Support in the Grid," *IECON 2018 - 44th Annual Conference of the IEEE Industrial Electronics Society*, Washington, DC, 2018, pp. 5574-5579.

[12] D. G. Shah, D, M. L. Crow, "Online Volt-Var Control for Distribution Systems With Solid State Transformers," *IEEE Trans. Power Del*, vol. 31, no. 1, pp 343 – 350, Feb. 2016.

[13] X. She, X. Yu, F. Wang and A. Q. Huang, "Design and Demonstration of a 3.6-kV–120-V/10-kVA Solid-State Transformer for Smart Grid Application," *IEEE Trans. Power Electron.*, vol. 29, no. 8, pp.3982-3996, Aug. 2014.

[14] S. Madhusoodhanan et al.,"Solid State Transformer and MV Grid Tie applications enabled by 15 kV SiC IGBTs and 10 kV SiC MOSFETs based Multilevel Converters", *IEEE Transactions on Industry Applications*, Vol.51, No. 4, July-Aug, 2015, pp3343-3360.

[15] G. D. Carne, G. Buticchi, Z. X. Zou, and M. Liserre, "Reverse power flow control in an ST-fed distribution grid," *IEEE Transactions on Smart Grid*, vol. PP, no. 99, pp. 1–1, 2017.

[16] A. von Jouanne, B. Banerjee, "Assessment of Voltage Unbalance", *IEEE Transactions on Power Delivery*, vol. 16, no. 4, Oct. 2001.

[17] R. M. Ciric, L. F. Ochoa, A. Padilla-Feltrin, and H. Nouri, "Foult analysis in four-wire distribtuion networks," Proc. Inst. Elect. Eng., Gen., Transm. Distrib., vol. 152, no. 6, pp. 977-982, 2005.

[18] S. Inoue, T. Shimizu, and K. Wada, "Control methods and compensation characteristics of a series active filter for a neutral conductor," *IEEE Trans. Ind. Electron.*, vol. 54, no. 1, pp. 433–440, Feb. 2007.

[19] B. Singh and J. Solanki, "An implementation of an adaptive control algorithm for a three-phase shunt active filter," *IEEE Trans. Ind. Electron.*, vol. 56, no. 8, pp. 2811–2820, Aug. 2009.

[20] O. Vodyakho and C. C. Mi, "Three-level inverter-based shunt active power filter in three-phase three-wire and four-wire systems," *IEEE Trans. Power Electron.*, vol. 24, no. 5, pp. 1350–1363, May 2009.

[21] P. Salmeron and S. P. Litrán, "A control strategy for hybrid power filter to compensate four-wires three-phase systems," *IEEE Trans. Power Electron.*, vol. 25, no. 7, pp. 1923–1931, Jul. 2010

[22] H. Akagi and T. Hatada, "Voltage balancing control for a three-level diode-clamped converter in a medium-voltage transformerless hybrid active filter," *IEEE Trans. Power Electron*., vol. 24, no. 3, pp. 571–579, Mar. 2009

[23] J. Wu, H. Jou, H. Hsaio, and S. Xiao, "A New hybrid power conditioner for suppressing harmonics and neutral-line current in three-phase four-wire distribution power systems," *IEEE Trans. Power Deli*., vol. 29, no. 4, Aug. 2014.

[24] A. E. Leon, J. M. Mauricio, J. A. Solsona, and A. Gómez-Expósito, "Adaptive control strategy for VSC-based systems under unbalanced network conditions," *IEEE Trans. Smart Grids*, vol.1, no.3 pp.311-319, Dec. 2010.

[25] M. Marwali, J. Jung, and A. Keyhani, "A three-phase four-wire inverter control technique for a single distributed generation unit in island mode," *IEEE Tran. Power Electron.*, vol. 23, no. 1, pp.322-331, 2008.

[26] G. Kim, C. Hwang, J. Jeon, J. Ahn and E. Kim, "A novel three-phase four-leg inverter based load unbalance compensator for stand-alone microgrid Author links open overlay panel," *International Journal of Electrical Power & Energy Systems*, vol. 65, pp. 70-75, Feb. 2015.

[27] S. Dasgupta, 1. V. Prasanna, S. K. Sahoo and S. K. Panda, "A novel four-leg three-phase inverter control strategy to reduce the data center thermal losses: elimination of neutral current", 38th *Annual Conference on IEEE Ind. Electron. Society* (IECON 2012), Montreal, QC, Canada, 25-28 Oct. 2012.

[28] Z. Guo, S. Panda and 1. V. Prasanna, "Design of new control strategies for a four-leg three-phase inverter to eliminate the neutral current under unbalanced loads", *Power Electron. Conference (IPEC-Hiroshima 2014-ECCE-ASIA*), Hiroshima, Japan, 18-21 May 2014.

[29] Copper Development Association "Voltage disturbances standard EN 50160- voltage characteristics in public distribution systems", Power Quality Application Guide, July 2004.

[30] J. Chen, T. Yang, C. O'Loughlin and T. O'Donnell, "Neutral Current Minimization Control for Solid State Transformers Under Unbalanced Loads in Distribution Systems," in *IEEE Transactions on Industrial Electronics*, vol. 66, no. 10, pp. 8253-8262, Oct. 2019.

[31] J. Chen, R. Zhu, M. Liserre and T. O'Donnell, "Neutral current reduction control for smart transformer under the imbalanced load in distribution system," *2018 13th IEEE Conference on Industrial Electronics and Applications (ICIEA)*, Wuhan, 2018, pp. 2381-2386.

[32] ANSI/IEEE Std 936-1987, "An american national sandard IEEE guide for self-cmmutated converters," *The Institute of Electrical and Electronics Engineers*, Inc 345 East 47th street, New York, NY 10017, USA, Jul. 1986.

[33] P. Pillay, M. Manyage, "Definitions of voltage unbalance," *Power Engineering Letters*, IEEE Power Engineering Review, May 2001.

[34] D. K. Alves, R. L. A. Ribeiro, F. B. Costa and T. O. A. Rocha, "Real-Time Wavelet-Based Grid Impedance Estimation Method," in *IEEE Transactions on Industrial Electronics*, vol. 66, no. 10, pp. 8263-8265, Oct. 2019.

[35] N. Hoffmann and F. W. Fuchs, "Minimal invasive equivalent grid impedance estimation in inductive resistive power networks using extended Kalman filter," *IEEE Trans. Power Electron*., vol. 29, no. 2, pp. 631–641, Feb. 2014

[36] S. Cobreces, E. J. Bueno, D. Pizarro, F. J. Rodriguez, and F. Huerta, "Grid impedance monitoring system for distributed power generation electronic interfaces," *IEEE Trans. Instrum. Meas*., vol. 58, no. 9, pp. 3112–3121, Sep. 2009.

[37] Copper Development Association "Harmonics neutral sizing in harmonic rich installation 3.5.1", Power Quality Application Guide, July 2003.

[38] A. Elaziz, A. Fatehy, K. Rushdy and N. Ahmed, "The analysis of magnification of neutral current In the presence of power quality problems," 23rd International Conference on Electricity Distribution, Lyon, paper 0344, 15-18 June 2015.

[39] I. Ibrahim, V. Rigoni, C. Loughlin, S, Jasmin and T. Donnell, "Real-time simulation platform for evaluation of frequency support from distributed demand response," *Cigre Symposium Dublin 2017*. Paper 162.

Junru Chen (S'17-M'20) received the ME and PhD degree in Electrical Energy Engineering from University College Dublin in 2016 and 2019. He was exchanging student at Kiel University (Germany) in 2018 and at Tallinn University of Technology (Estonia). He is currently a Senior Researcher at University College Dublin and a Visiting Scholar at Aalborg University, Denmark. His current research interests in Power electronics control, modelling, stability and application.

Rongwu Zhu (S'12-M'15) received the B.Eng. in Electrical Engineering from Nanjing Normal University, Nanjing, China, in 2007 and Ph.D. degree in energy technology from Department of Energy Technology, Aalborg University, Aalborg, Denmark, in 2015. From 2011-2012, he was a guest researcher with Aalborg University. He is currently a Senior Research with Chair of power electronics, at Christian-Albrechts-University of Kiel (Germany).

He has authored and co-authored over 85 technical papers (over 1/3 of them in international peer-reviewed journals). His research interests include renewable power generation, operation and control of electric grid with high penetration of renewables, reliability and resilience improvement of power electronics dominated grid.

Ismail Ibrahim recieved B.Tech degree from National Institute of Technology, Tiruchirapalli, India in 2010 and M.E in2015 and PhD in 2020 from University college Dublin, Ireland all in electrical engineering. He joined Eirgird in 2020 as senior innovation engineer. His research interests are Power Electronics Converters, Power system studies, Renewable Integration and Distributed Energy Resources.

Terence O'Donnell (M'96-SM'20) is an associate professor in the School of Electrical and Electronic Engineering in University College Dublin. He is a principle investigator within the UCD Energy Institute where his research interests are focused on the use of power electronics converters in power systems and in particular on the interfacing of power electronics to the grid. Specific interests include the grid applications of solid state transformers, the control of

converters for distributed energy resources and the use of power hardware in the loop testing methods.
Terence has previously worked in the Tyndall National Institute in Cork where he has worked on numerous research projects, both at national and international level, relating to design, modelling and fabrication of magnetics for power conversion, magnetic field sensors, inductive powering and energy harvesting. Terence is an author on over 50 publications in peer reviewed journals.

Marco Liserre (S'00-M'02-SM'07-F´13) received the MSc and PhD degree in Electrical Engineering from the Bari Polytechnic, respectively in 1998 and 2002. He has been Associate Professor at Bari Polytechnic and from 2012 Professor in reliable power electronics at Aalborg University (Denmark). From 2013 he is Full Professor and he holds the Chair of Power Electronics at Kiel University (Germany). He has published 500 technical papers (1/3 of them in international peer-reviewed journals) and a book. These works have received more than 33000 citations. Marco Liserre is listed in ISI Thomson report “The world’s most influential scientific minds” from 2014.
He has been awarded with an ERC Consolidator Grant for the project “The Highly Efficient And Reliable smart Transformer (HEART), a new Heart for the Electric Distribution System”.
He is member of IAS, PELS, PES and IES. He has been serving all these societies in different capacities. He has received the IES 2009 Early Career Award, the IES 2011 Anthony J. Hornfeck Service Award, the 2014 Dr. Bimal Bose Energy Systems Award, the 2011 Industrial Electronics Magazine best paper award and the Third Prize paper award by the Industrial Power Converter Committee at ECCE 2012, 2012, 2017 IEEE PELS Sustainable Energy Systems Technical Achievement Award and the 2018 IEEE-IES Mittelmann Achievement Award.